Research and Implementation of a USB Interfaced Real-Time Power Quality Disturbance Classification System

Mehmet GÖK[1], İbrahim SEFA[2]
[1]*Karabuk University, Balıklar Kayası Mevkii Demir Çelik Kampüsü, Karabük, Turkey*
[2]*Gazi University, 06500 Teknikokullar, Ankara, Turkey*
2011638126002@ogrenci.karabuk.edu.tr

***Abstract*—In this study, the research and implementation of an automatic power quality (PQ) recognition system are presented. This system contains a USB interfaced multichannel data acquisition (DAQ) device and a graphical user interfaced (GUI) application. The DAQ device consists of an analog-to-digital (ADC) converter, field programmable gate array (FPGA) and a USB first in first out (FIFO) buffer interface chip. The application employs Stockwell Transform (ST) technique combined with neural network model to build the classifier. Eight basic and two combined PQ disturbances are determined for the classification. Different from the previous studies, the synthetic signals used for neural network training are modified by adding the harmonics detected in the real signal. This approach is used to increase the classifier accuracy against the real line power signal. Also, ST is simplified by using only the frequencies which are required in the feature extraction step to reduce the processing time. Developed application handles the signal processing, the classification, and the database recording tasks by using multi-threaded programming approach under the mean time of 41 ms. The experimental results show that the proposed power quality disturbance detection system is capable of recognizing and reporting power quality faults effectively within the real-time requirements.**

***Index Terms*—discrete transforms, graphical user interfaces, neural networks, power quality, real-time systems.**

I. INTRODUCTION

Different types of non-linear loads such as controlled and non-controlled rectifiers, AC voltage controllers and saturated inductive loads are several of the most common causes of the increasing voltage or current signal distortion. The distortions lead to produce different types of power quality (PQ) symptoms. In recent years, those disturbances take more attention because of having negative effects on power sensitive equipment used in industrial plants. PQ faults must be detected, analyzed and classified to take necessary preventive measures. These tasks should be taken to reduce the economic losses caused by such power quality problems.

In a secure power electric system, voltage and current waveforms should be monitored and acquired continuously in order to detect the disturbances effectively. Captured data are analyzed and classified using appropriate digital signal processing and machine learning methods. Digital signal processing techniques such as Wavelet Transforms (WT) [1-5] and ST [2], [6-14] have a widespread application area in the literature. These methods are used to extract a pattern that characterizes different PQ disturbances. Machine learning methods such as Artificial Neural Networks (ANN) [1], [2], [7-9], decision trees (DT) [3-4], [11], [15-17], and Support Vector Machines (SVM) [18-19] are used to address the pattern to related PQ disturbances.

There are many powerful automatic power quality detection and recognition systems developed by using mentioned methods [19], [20]. Costly and complex designs and low modularity can be counted as common drawbacks of such systems. There are some studies using LabVIEW virtual instrumentation packages [14], [21-23] and dSPACE systems [10]. These solutions provide researchers with powerful components to evaluate the signal processing algorithms. However, the highly developed hardware [24] and software dependencies can be considered as drawbacks of these systems. This dependency may lead issues when portable end-user instrument design is desired. Also, there are other studies on automatic power quality disturbance classification systems employing digital signal processor (DSP) and field programmable gate array (FPGA) solutions [25-26]. These systems are highly effective solutions with high performance. However, these solutions need an external computer with general purpose processor for database and networking operations. The studies [27-28] propose complete system approaches for an embedded power quality recognition system. Nevertheless, high hardware design complexity can be considered drawbacks for these studies.

This paper demonstrates the research and implementation of a relatively inexpensive and practical real-time power quality recognition system. The system design contains a USB interfaced data digitizer hardware and a single board computer compatible software used to detect and to classify the PQ disturbance. The proposed system processes three-phase voltage signals to realize classification tasks. The signal processing software uses ST for feature extraction and ANN for PQ disturbance classification. All of the classified disturbance other than normal is recorded into structured query language (SQL) compatible database for a possible further assessment. The main contribution of this paper is to present an affordable real-time power quality classification methodology by using a simplified ST scheme with the platform independent hardware and software.

Digital Object Identifier 10.4316/AECE.2017.03008

II. System Overview

The classification system acquires three-phase power signal data by using the USB interfaced data acquisition device. Voltage signals are sampled at 10 ksps and 5 periods of the signal are used to detect and classify the possible PQ disturbance (PQD). Acquired signal data are organized as windows which are five periods length. Each window is plotted in the GUI of the application. Then ST operation is performed over the window. The amplitude matrix is calculated after ST operation. Seven types of features comprising the recognition pattern is calculated. The recognition pattern is fed into ANN and the output is monitored. If the maximum output value is observed at a different output rather than Output 0 (output for a NORMAL situation), the classification result (fault type), time and raw signal data are recorded into SQL database table. The raw signal data may be used for post-process assessment if necessary. The flowchart of the classification task is shown in Fig. 1.

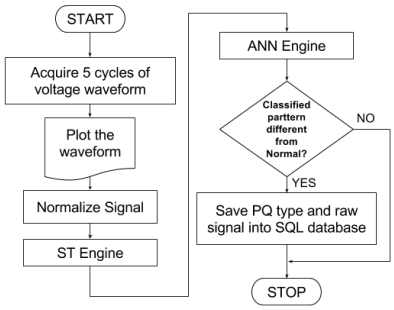

Figure 1. Flowchart showing the proposed classification process

III. Design of Data Acquisition (DAQ) Device

DAQ unit is used to digitize AC power signal and transmit the obtained data to the computer. Its capture rate can be set up to 200 ksps for all 8 channels. This device is the enhanced version of our previous design proposed in [29]. In this design, Xilinx Spartan 6 FPGA is used instead of the microcontroller to control data acquisition. DAQ unit employs three components: Spartan 6 FPGA board (Papilio Pro), AD7606 Analog-to-Digital converter breakout board and FT2232H USB-FIFO interface breakout board (Fig. 2).

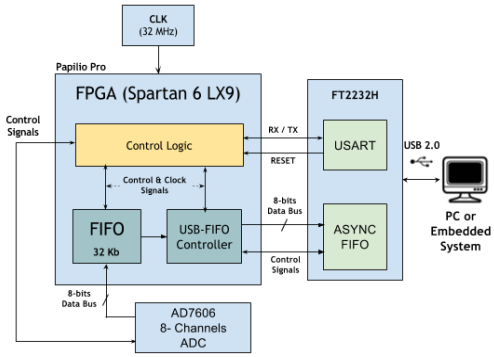

Figure 2. Block scheme of proposed USB interfaced data digitizer device

FT2232H is used for buffering and transmitting sampled data through the USB port. FT2232H is a dual channel USB UART/FIFO interface chip. Channel A of FT2232H is programmed as UART and channel B is programmed as asynchronous FIFO mode. UART channel is used to send a command to FPGA control logic: start sampling, stop sampling and set sampling rate. FIFO channel is used for transmitting raw signal data to the computer.

AD7606 is a 16-bit successive approximation (SAR) ADC with 8 channels synchronous sampling. The AD7606 comes with the following features that make it an ideal part for data acquisition systems (DAS):

- Sampling rate up to 200 ksps on all channels,
- Bipolar analog input ranges from ±5 V to ±10 V,
- Single 5 V analog supply,
- Analog input clamp protection,
- Second-order antialiasing analog filter,
- Flexible parallel/serial interface.

AD7606 has been used for different applications [26], [28-31] requiring accurate data acquisitions from power quality detection to vibration sensing.

The FPGA configuration is designed using Xilinx ISE 14.7. The configuration bitstream is transferred to FPGA by using JTAG interface channel of an onboard FT2232D chip. Project tree is given in Fig. 3.

Figure 3. Xilinx ISE project tree of the DAQ device configuration

In the project tree, pp_ft2232_top is the Verilog module (top-level module) that interconnects the other modules. This can be considered as a virtual motherboard like in a personal computer hardware. The functions of the other modules are briefly described below:

PwmGen: This module is used to generate 10 KHz sampling signal from 32 MHz crystal oscillator on Papilio Pro board. This module outputs a pulse width modulation (PWM) signal with 50% duty cycle.

Frequency_divider_by2: This module is used to generate the read signals for ADC and the write signals for the internal FIFO by dividing 32 MHz clock signal by 2.

aFifo: It is the memory used for buffering ADC data before sending it through the USB interface. This is derived using FIFO IP Core provided by Xilinx in ISE Design Suite. It operates in asynchronous mode and read/write speed is 16 MHz.

Async_sender: This module is used to transfer ADC data from aFIFO to the data stream channel of USB-FIFO (Channel B).

Daq_interface: This module is used to start and to stop the sampling operation. The sub-module serial_rx is used to read the command comes from the computer side. serial_rx reads the command data at 2 MBaud communication speed. This module reads the commands through Channel A. RTS (Ready-to-Send) pin of UART module is used to reset FPGA modules and ADC.

All the FPGA modules operate in parallel when the acquisition is active. For example, when the command of stop sampling is sent over UART; sampling, reading and writing operations are not interrupted. The device's tested data throughput is 40 ksps x 2 bytes x 8 channels = 625 kb/s. This amount of data can be transmitted through USB-FIFO without any bottlenecks because the maximum asynchronous data transfer rate of FT2232H is 8

Megabytes/second. TXE flag of the FT2232H is checked before writing. This flag indicates whether the on-chip transmit buffer is full or not. When the device driver is late to read from the on-chip buffer, the data coming from ADC is accumulated into FIFO buffer inside FPGA. The data stream is ensured in this way.

The proposed device draws only 100 mA current and does not require any additional components for data acquisition control management. Reference [32] proposes a competitive device that uses MAX11046 ADC, FT2232H and a complex logic programmable device (CPLD). Additionally, this design employs a microcontroller (PIC12F509) for the data acquisition control, which brings the requirement of additional firmware development. This device also draws 300 mA current, thus consumes more power than proposed device. The main contribution of this section is to present how an FPGA can be efficient for portable, flexible, low cost and low power consumption instrumentation design.

IV. Design of Proposed Data Analysis Pipeline

In this section, PQD classification steps are explained. Firstly, ST is described. Secondly, feature extraction method is presented. Then the generation of PQ disturbances used in this study is explained. This section ends with the discussion about the classification of the PQ disturbances and previous studies.

A. Stockwell Transform

The mathematical representation of ST is presented by Stockwell *et al.* [33] by using Wavelet transform (WT) and Short Time Fourier Transform (STFT). The Continuous wavelet transform (CWT) of the input signal *h(t)* is defined as in (1) [9], [14], [17], [18], [34]:

$$W(\tau,d)=\int_{-\infty}^{\infty}h(t)w(t-\tau,d)dt \tag{1}$$

where *w(t-τ, d)* is the scaled form of the fundamental wavelet. The parameter *d* is the scaling factor that is obtained by inverting the fundamental frequency of the input signal. The ST of function *h(t)* is defined as a CWT with a specific mother wavelet multiplied by the phase factor (2)

$$S(\tau,f)=e^{j2\pi ft}W(\tau,d) \tag{2}$$

where the mother wavelet for this phase corrected equation is defined as in (3):

$$w(t,f)=\frac{|f|}{\sqrt{2\pi}}e^{-\frac{t^2f^2}{2}}e^{-j2\pi ft} \tag{3}$$

The equation (3) is not a CWT due to the lack of having a zero mean condition for an acceptable wavelet. Final equation of the continuous S-transform is obtained by using the inverse of *f* as dilation parameter as in (4):

$$S(\tau,f)=\int_{-\infty}^{\infty}h(t)\frac{|f|}{\sqrt{2\pi}}e^{-\frac{(\tau-t)^2f^2}{2}}e^{-j2\pi ft}dt \tag{4}$$

The ST can also be expressed as the operations on the Fourier spectrum *H(f)* of *h(t)* as written in (5):

$$S(\tau,f)=\int_{-\infty}^{\infty}H(\alpha+f)e^{-\frac{2\pi^2\alpha^2}{f^2}}e^{j2\pi\alpha\tau}d\alpha, f\neq 0 \tag{5}$$

The power system signal *h(t)* can be expressed in a discrete form as *h(kT)*, *k=0,1,..,N-1* where *T* is the sampling interval and *N* is the total samples number. The discrete Fourier transform (DFT) of *h(kT)* is expressed as in (6):

$$H\left[\frac{n}{NT}\right]=\frac{1}{N}\sum_{k=1}^{N-1}h(kT).e^{(-\frac{j2\pi nk}{N})} \tag{6}$$

where *n=0,1,..,N–1*. Using (5), the ST of a discrete time series *h(kT)* is given by (let $\tau\rightarrow kT$ and $f\rightarrow n/nT$) as in (7) [9], [14], [17], [32].

$$S\left[kT,\frac{n}{NT}\right]=\sum_{m=0}^{N-1}H\left[\frac{m+n}{NT}\right]e^{-\frac{2\pi^2m^2}{n^2}}e^{\frac{j2\pi mk}{N}}, n\neq 0 \tag{7}$$

where *k, m=0,1,..,N-1*, and *n=1,..,N-1*. For *n=0* (the frequency at zero) the transform is done by calculating the mean of amplitudes in the frequency spectrum (8) [17], [18].

$$S[kT,0]=\frac{1}{N}\sum_{m=0}^{N-1}h\left(\frac{m}{NT}\right) \tag{8}$$

The ST localizes both the phase spectrum and the amplitude spectrum. By using FFT, convolution and inverse FFT, the discrete ST can be computed fast. The output of ST is a complex matrix whose rows and columns are frequency and time values, respectively. ST-amplitude matrix (STA) (9) is calculated to analyze power signal disturbances, in which the rows are the frequencies and the columns are the time samples [7], [17], [33].

$$A(kT,f)=\left|S\left[kT,\frac{n}{NT}\right]\right| \tag{9}$$

The information contained in the time-frequency spectrum (each row in STA-matrix) is used to analyze and determine the PQ disturbance (PQD) characteristics in this paper. The graphical representation of the STA exhibits frequency-time, amplitude-time, and frequency amplitude plots. In this study, for the pre-processing step ST is preferred. Because ST is immune to noisy conditions and preserves phase information of analyzed signal [14], [17].

B. Feature Extraction

By observing the frequency rows (contours) of STA, the distinctive features of PQDs can be determined easily. A distorted power signal with oscillatory transient and 5th harmonic is given in Fig. 4 (a) and 150 Hz, 250 Hz, 350 Hz and 700 Hz contours in (b) to (e), respectively [11], [20]. It can be seen that the oscillatory transient triggers the energy existence at 700 Hz contour (e). Also, there is a big energy concentration response to the existence of 5th harmonic at 250 Hz contour at the end of the signal. These concentrations corresponding to different disturbances present distinctive features.

In Fig. 5, a signal with interruption and several frequency contours are given. The contour related to 50 Hz is noted to decrease its value during the interruption. The other frequency contours exhibit a low energy at the beginning and at the end of interruption. In these examples, it can be seen that the transient events (e.g. beginning of interruption or oscillatory transient) can be detected by examining high-order harmonics. In addition, any harmonics event can be detected by searching corresponding frequency contours [2], [11], [20].

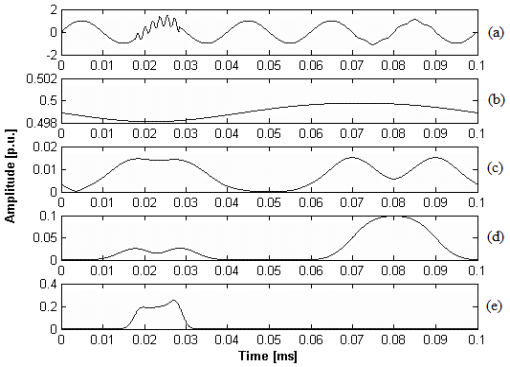

Figure 4. Signal with an oscillatory transient and 5th harmonic (a). 50 Hz contour (b), 150 Hz contour (c), 250 Hz contour (d), 700 Hz contour (e) [20]

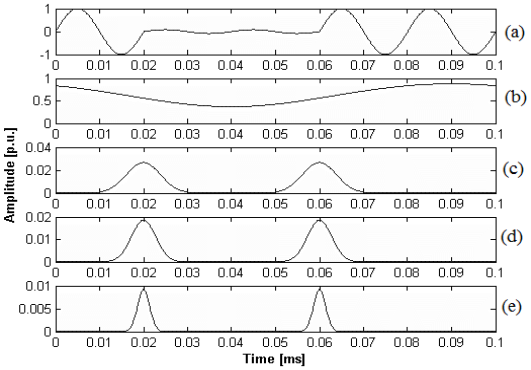

Figure 5. Voltage interruption (a). 50 Hz contour (b), 150 Hz contour (c), 250 Hz contour (d). 700 Hz contour (e)

In this paper, the distinctive features are extracted by using these advantages provided by STA contours. The 50 Hz contour presents useful information about sags, swells, and interruptions [2], [34]. Thus, the mean value of 50 Hz contour has been selected as a distinctive feature. However, this feature does not clearly distinguish between sags and interruptions, and therefore, there is a need for another feature. The second and the third features are obtained by determining the minimum and the maximum absolute peak values of the sinusoidal power signal (Fig. 6). In the previous work [11], the minimum value of 50 Hz contour selected to distinguish sag and interruption cases. Nevertheless, this feature is not enough as seen in sag and interruption classification accuracy with PSCAD generated data as seen at the end of same work.

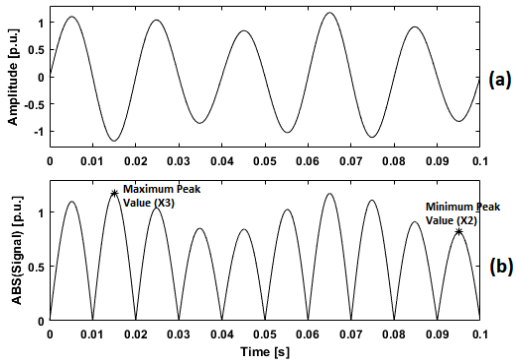

Figure 6. Signal with Flicker (a), absolute value of the signal and selected features X2 and X3 (b)

In order to detect the disturbances including the third, the fifth and the seventh harmonics, the mean value of contours related to these frequencies (150 Hz, 250 Hz, and 350 Hz) are used. Mean values of these contours are preferred due to the requirement of lower computation burden compared to the energies used in [11], [20].

The sum of mean values for contours from 600 Hz to 1600 Hz has been selected as another characteristic feature. The value of this feature gives information about the high frequency transient events like an oscillatory transient.

The features constituting the recognition pattern are summarized in Table I. The features X1, X4, X5, X6, and X7 are extracted from the rows of STA. Therefore, ST is applied over these rows (frequencies). There is no need for operation of full spectrum ST.

TABLE I. THE FEATURES COMPRISING THE RECOGNITION PATTERN

Feature	Description
X1	Mean of 50 Hz contour
X2	Minimum peak value of 5 cycles
X3	Maximum peak value of 5 cycles
X4	Mean Value of 150 Hz Contour
X5	Mean Value of 250 HZ Contour
X6	Mean Value of 350 Hz Contour
X7	Sum of mean values from 600 Hz to 1600 Hz

C. PQ Disturbance Generation

In this paper, the classification work for eight types of simple and two types of combined power quality disturbances are realized: the simple PQDs are swell, sag (dip), interruption (outage), oscillatory transient, harmonics, flicker, notching; combined PDQs are swell with harmonics and sag with harmonics. Class labels belong to these disturbances are given in Table II.

TABLE II. CLASS LABELS BELONG TO DISTURBANCES

Disturbance	Label
Normal	C1
Sag	C2
Swell	C3
Interruption	C4
Harmonics	C5
Oscillatory Transient	C6
Flicker	C7
Sag+Harmonics	C8
Swell+Harmonics	C9
Notching	C10

The signals related to these disturbances are generated by using MATLAB according to power signal disturbance models [1], [5], [23], [35] based on IEEE 1159 standards. These synthetic signals are sampled at 10 ksps within five cycles. Evaluated power system's fundamental frequency is 50 Hz and the normalized voltage peak value is 1 V.

These signals are modified by adding the harmonics that are measured with our previous system proposed in [29]. This modification is performed to enhance the classifier accuracy against the real power signal. This modification is applied to 40% of the signals that are generated for training. The harmonics and their amplitudes added to the synthetic signals are shown in Table III. The features given in Table I, are extracted by using these signals. Then the ANN is trained by using these features.

TABLE III. HARMONIC AMPLITUDES ARE ADDED TO SIGNAL MODELS

Frequency	Amplitude
150 Hz	0.056379
250 Hz	0.06528
350 Hz	0.014343
450 Hz	0.008286

Fig. 7 shows the scatter plot of feature values X2 versus X3 of test patterns for Normal, Sag, Swell and Interruption classes. These classes are distinguished well by these features. Fig. 8 shows the scatter plot of feature values X3 and X7 of test patterns for Harmonics, Oscillatory Transient, Flicker, Sag+Harmonics, Swell+Harmonics and Notching classes. Sag+Harmonics and Notching classes have some overlapping cases.

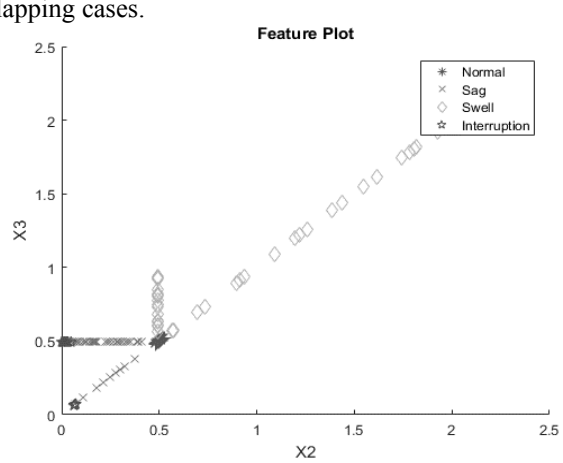

Figure 7. Scatter plot of feature values X2 versus X3 of test patterns for Normal, Sag, Swell and Interruption classes

The ANN classifier eliminates this ambiguity with the contribution of features X2 and X4 as seen in Fig 9. In this plot, Swell+Harmonics and Notching classes have some overlapping cases.

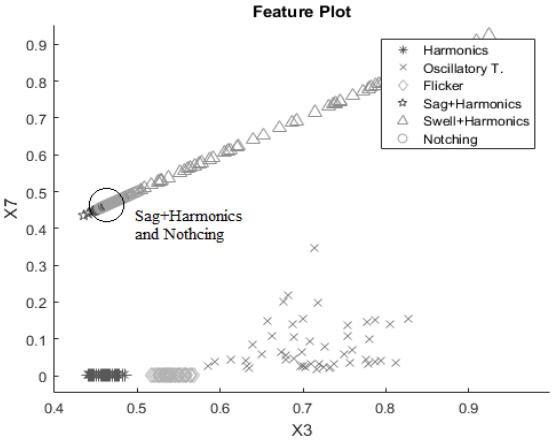

Figure 8. Scatter plot of feature values X3 and X7 of test patterns for Harmonics, Oscillatory Transient, Flicker, Sag+Harmonics, Swell+Harmonics and Notching classes

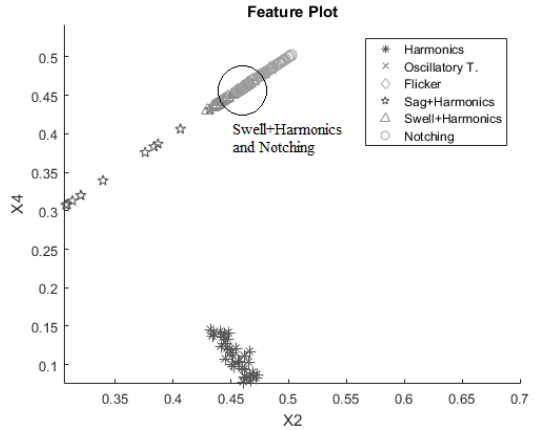

Figure 9. Scatter plot of feature values X2 and X4 distinguishing Notching and Sag+Harmonics classes

D. PQD Classification By Use Of ANN

Neural networks have been used as an important tool for classification, and have been applied to wide range of real world tasks successfully [36]. It has been used as a PQD classification tool in different studies [2], [37].

In this paper, feedforward backpropagation ANN is used to classify PQDs. The ANN has two layers: hidden layer and output layer. The number of neurons in the hidden layer is determined as a function of number of inputs, regarding the expression (2n+1), where *n* is the number of inputs to the ANN [2]. The transfer function between input and hidden layer is *tansigmodial*; the transfer function between the hidden and the output layer is lineal. The learning ratio is determined as 0.07, the epoch 100000 and the training algorithm is selected as *traingd*. The implementation is performed using MATLAB.

ANN is trained with the signal data according to the signal models mentioned in the previous subsection. 50 signals are generated for each disturbance type (Totally 500 signals are generated for training set). Then ST is applied to these signals. The features given in Table I are extracted after ST. Input matrix to be used for ANN training is constructed with these features. ANN is trained with the input matrix (500x7) by using given parameters above. After the training operation is completed ANN is saved (Fig. 10 (a)).

For the validation of the ANN and selected features, 500 signals are generated with random parameters again. Features of these signals are extracted and tested with pre-trained ANN. For every step of the validation, the confusion matrix is updated (Fig. 10 (b)). Classification accuracy is calculated from the confusion matrix. By using this method, a classification accuracy of 98.4% is obtained with synthetic signals. However, we observe that the ANN fails against the real signal disturbances. For example, recorded normal signal including low level harmonics is classified as harmonics.

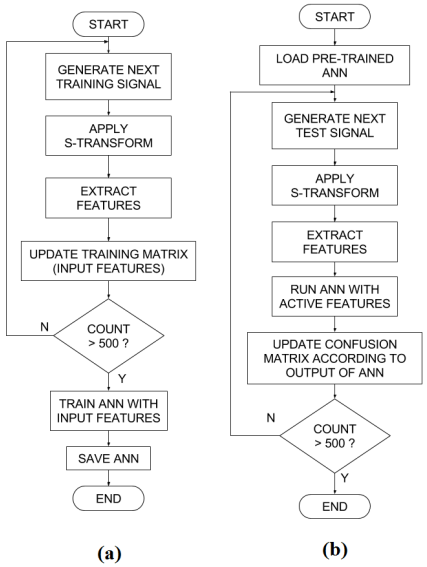

Figure 10. Training (a) and verification (b) flowcharts of the ANN

For better validation of the ANN against the real signal data, 500 signals are generated with random parameters again. Harmonics measured in real (as given in Table III) signal are added to these signals. After the validation, a

classification accuracy of 80% is obtained. This accuracy rate shows that the real signal harmonics have negative effects on classification accuracy. Therefore, ANN is re-trained with harmonics injected signals. When network training is completed after 100000 iterations, mean square error (MSE) is obtained as 0.0293. Validation is repeated with harmonics injected new test data and a classification accuracy of 94.7% is obtained. The confusion matrix for this evaluation is given in Table IV. Diagonal elements of the table indicate true classifications and the other elements indicate misclassifications. As seen in Table IV, sag (C2) case is misclassified as interruption for 6 times for the worst situation.

TABLE IV. CONFUSION MATRIX OBTAINED USING ANN WITH PROPOSED FEATURES

	C1	C2	C3	C4	C5	C6	C7	C8	C9	C10
C1	50	0	0	0	0	0	0	0	0	0
C2	5	**39**	0	6	0	0	0	0	0	0
C3	1	0	43	0	0	3	3	0	0	0
C4	0	3	0	47	0	0	0	0	0	0
C5	0	0	0	0	50	0	0	0	0	0
C6	0	0	0	0	0	50	0	0	0	0
C7	1	0	0	0	0	0	49	0	0	0
C8	0	0	0	1	6	0	0	43	0	0
C9	0	0	0	0	1	0	0	0	49	0
C10	0	0	0	0	0	0	0	0	0	50
Overall Accuracy									**94.7%**	

Precision, Recall and F measure values extracted from the confusion matrix, is given in Table V. According to F measure results, the overall accuracy rate is almost reasonable for the accuracy rate of each class except the C2. Recall value (0.78) for C2 shows that the disturbance of sag is misclassified more times than the other classes. This classification error can be reduced by enhancing the samples of the related perturbations.

The main contribution of this section is to reveal that the classification accuracy of a power quality classifier ANN can be enhanced by using the real signal harmonics in the training step. Example MATLAB codes for training and test stages can be accessed from GitHub repository: https://github.com/pqd-researcher/pqd_class_verification.

TABLE V. PRECISION, RECALL AND F MEASURE VALUES OBTAINED FROM CONFUSION MATRIX

	C1	C2	C3	C4	C5	C6	C7	C8	C9	C10
Precision	0.88	0.93	1.00	0.87	0.88	0.94	0.94	1.00	1.00	1.00
Recall	1.00	**0.78**	0.86	0.94	1.00	1.0	0.98	0.86	0.98	1.00
F measure	0.93	**0.85**	0.92	0.90	0.93	0.97	0.96	0.92	0.99	1.00

Levenberg-Marquardt backpropagation algorithm (trainlm) is also tested within our study. MSE is obtained as 0.00175 after 39 iterations with this method. Convergence of this method is much faster than gradient descent approach. Nevertheless, a verification accuracy of 87% is obtained with the ANN trained by use of the Levenberg-Marquardt algorithm.

Comparison of S-Transform based classification schemes are given in Table VI. Uyar *et al.* [7] obtained very high accuracy with synthetic signal data by using ANN. Authors of that paper used 14 features that may be challenging for real-time implementation. Biswall and Dash [10] obtained very high accuracy by using DT with real signal data acquired from a laboratory setup. However, the number of features required for classification is relatively high as in reference [7]. Li and Chilukuri [18] used SVM with particle swarm optimization (PSO) for classification. In this paper, the number of classified PQDs is low in comparison to other studies. Rodriguez *et al.* [20] used a rule based (RB) approach to classify the disturbances. They tested the method with synthetic signals at different noise levels. Classification accuracy (99.5%) of RB approach is higher than ANN accuracy (98.4%) for signals with no noise. However, the classification accuracy of RB approach is lower (72.7%) than ANN accuracy (89%) for signals with the noise level of 20 dB.

TABLE VI. COMPARISON OF S-TRANSFORM PERFORMANCE WITH DIFFERENT CLASSIFIERS

Reference	**Type of Classifier**	**Type of Data**	**No. of Features**	**No. of PQ Disturbances**	**Accuracy**
Uyar *et al.* [7]	NN	Synthetic	14	9	99.67%
Biswall and Dash [15]	Decision Tree	Real	20	13	94.8%
Li and Chilukuri [18]	PSO-SVM	Synthetic	5	7	99%
Rodriguez *et al.* [20]	Rule Based Approach	Synthetic	6	11	99.5%
Kumar *et al.* [23]	NN + Decision Tree	Synthetic	5	13	99.9%
Mishra *et al.* [38]	PNN	Synthetic	4	11	94.7%
Lee and Dash [39]	PNN + Rule Based Decision	Synthetic	3	10	95.33%
Chilukuri and Dash [40]	Fuzzy	Synthetic	5	7	99.28%
Proposed Method	**NN**	**Synthetic+ Real Signal Harmonics**	**7**	**10**	**94.7%**

Kumar *et al.* [23] used DT and ANN combined classification scheme that can be hard to implement with a real-time classification system. Authors of paper [38] used the probabilistic neural network (PNN) to classify the PQDs. PNN is preferred in that study because of having a simple and adaptable structure with a fast learning stage. However, two of the features used in this study are column based features. These features may require the inspection of full-spectrum STA calculation. Lee and Dash [39] used rule based decision tree with PNN. Using combined classifier helps with enhancing the classification accuracy but brings more computational overhead as in [23]. Chilukuri and Dash [40] proposed a classification scheme based on Fuzzy rules. They obtained very high accuracy (99.28%) with synthetic signals at an SNR level of 40 dB. Nevertheless, the number

of PQDs is low as in [18]. The Fuzzy model, a widely used solution in control systems [41], [42], has also been used for detection and classification purposes in different applications [43], [44]. In addition to this, Fuzzy models, have also been employed to detect the PQDs [10], [35], [40].

The classification accuracy in these studies varies according to the number of features and the classified PQDs as well as the methods. As seen in the literature overview, neural network approach is more common and reliable for PQD recognition. In general, simulated signal data has been used for training and evaluation. Different from the previous studies, the main contribution of this section to present a method to deal with real power signal data by mixing harmonics with simulation data. In addition to this, the features used in recognition process are based on STA matrix rows (frequencies). ST calculation can be simplified by using only the required frequencies in recognition pattern instead of the full spectrum. Obtained accuracy with selected features shows that the proposed method is admissible for an online PQD recognition system.

V. Design of PQ Disturbance Classification Software

The classification software processes the digitized signal data and makes a decision about the PQD state. If a disturbance detected on one of the three phases, recognized PQ disturbance and five periods of signal data (1000 sample points) are recorded into Structural Query Language (SQL) compatible database. Also, the voltage signals can be monitored using graphical user interface (GUI) of the software. All these tasks are performed using three threads. The first thread is the main thread of the Qt application. This thread has the function to display and react to the graphical user interface. The second thread reads the data from the USB-FIFO buffer into processing queue of the software. The third thread reads the data from the processing queue and performs the required operations to plot and to classify the signal.

Data reader thread checks and reads the data package (3200 bytes for one period) from USB-FIFO, and then appends the data to the processing queue. The application reads FIFO buffer at the end of the power line signal period. *FT_GetStatus* Application Programming Interface (API) function is used to check whether the number of bytes exceeds 3200. This value indicates the period limit of the acquired signal for 8 channels at 10 ksps sampling rate. *FT_Read* function is used to read the buffered data (Fig. 11).

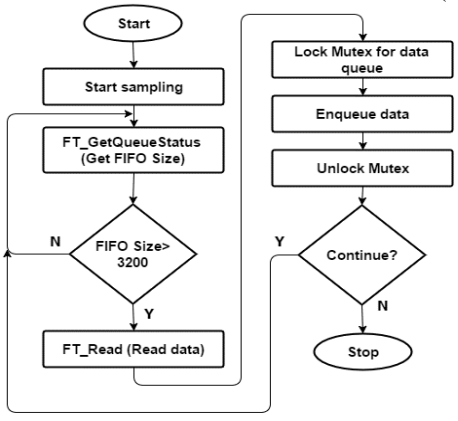

Figure 11. Flowchart for the Data Reader thread

Data processor thread reads the data back from the queue. The sampled data are read from the ADC in the ascending channels order. Therefore, data processor thread parses data into appropriate channels then performs the calculations and the display operations (Fig. 12).

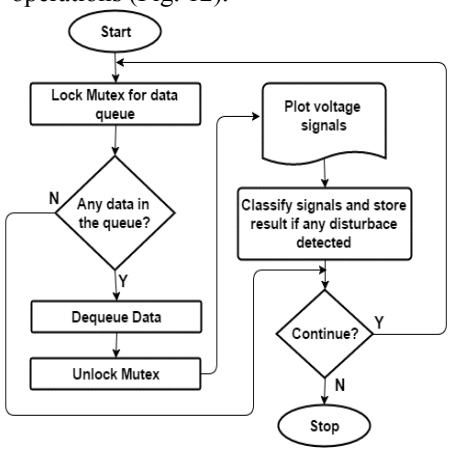

Figure 12. Flowchart for the Data Processor thread

Those threads are synchronized by using mutex mechanism. To keep the processing time under 100 ms deadline, thread priorities of those threads set to high by using setPriority call of Qt framework. Signal plotting operations are implemented with QtCharts. QtCharts comes with OpenGL ES 2.0 API support. Plotting task is offloaded from CPU to GPU with high performance operation by using OpenGL support. While the proposed software processes and makes a decision about the acquired data, incoming data is placed into the FIFO buffer by the device driver of FT2232H.

Acquired signal data is normalized to 1V peak value using a variable coefficient. This is a calibration task to catch the normal condition of the monitored power line. The coefficient can easily be changed by using a slider component in the GUI of the application (Fig. 13). DC part is removed from the acquired signals before S-Transform operation. AD7606 has a 2nd order anti-alias analog filter, therefore, the acquired signal is not filtered.

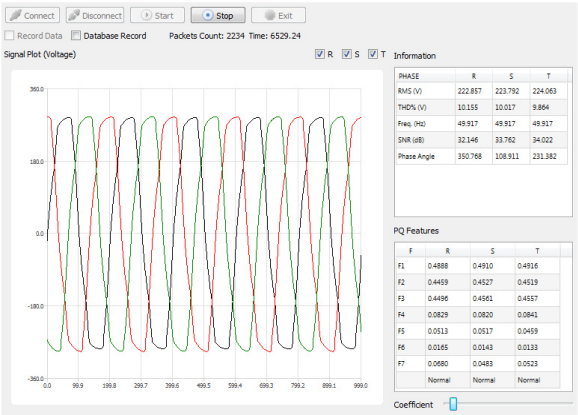

Figure 13. GUI of the proposed application

In this study, ST, is only performed over frequency rows that are used in the feature extraction step, instead of the full spectrum. Thus, 1 forward and 21 inverse DFT operations are performed for one phase of the power signal (Fig. 14). This approach makes the ST more suitable in real-time operations. He *et al.* [33] uses dynamics method to remove

unwanted frequencies from ST operation. A fast dyadic frequency scaling scheme is used to decrease computational burden of ST [15]. Such methods may require considering a different number of features varying according to different PQDs. This uncertainty makes the extraction process a bit more complicated. As proposed in this work, the fixed number of features preference is a simpler approach and more suitable for ANN classifier. The main contribution of this section is to present a way to reduce the computation time of ST by excluding unneeded frequency rows from the calculation.

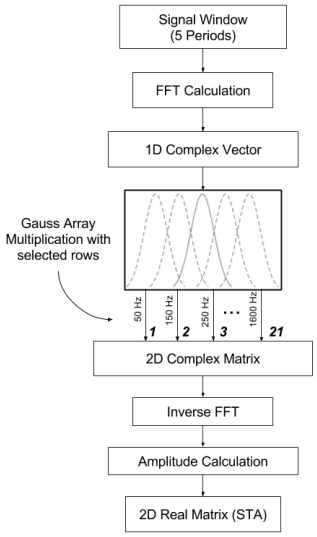

Figure 14. ST calculation with only selected frequencies

The gaussian window is pre-calculated at the application startup to reduce the runtime of ST by using a similar approach as used in [33]. DFT operations demanded by ST, are performed by using FFTW [45] library. All FFT plans within the application, are distributed into two threads to take the advantage of multi-core processor technology.

In the PQ disturbance classifier application, the neural network weights obtained in MATLAB application are used. After the training operation, the input layer and the bias weights (*W1* and *B1*) and the hidden layer and the bias weights (*W2* and *B2*) are exported as a single disk file. The PQD classifier application loads the weights from the file at startup. Classification is realized by two matrix multiplication operations using these weights and the feature vector by (10).

$$Y = B2 + W2 * \tanh(B1 + W1 * X) \qquad (10)$$

where Y is the output vector of the ANN and X is the input feature vector.

Example PQD events detected and recorded by the proposed system with real line signals are given in Fig. 15 and Fig. 16. The signal given in Fig. 15 demonstrates a flicker case. This signal is classified as flicker by the proposed application. Fig. 16 shows a swell case. This signal is classified as swell. Fig. 17 depicts a combined PQD with oscillatory transient and swell cases. This signal is classified as oscillatory transient. This event was detected during a monitoring session of an uninterruptible power supply (UPS) output on low battery. These classification results prove the robustness of the proposed system against real signal data.

The proposed application employs SQLite 3.0 database to store the information regarding PQ perturbations. SQLite database engine is built within Qt Library. Every PQ disturbance information detected by the application is inserted into regarding table in the database structure. Record row comprises of disturbance date, time, type and 5 cycles of raw signal. The raw signal data for three-phase take place in the separate columns in the record row.

The libraries used in the application project are open-source and come with the cross-platform support. By taking the advantage of these features, the application can easily be ported to Linux based operating systems and Mac OS X platforms. The project is designed by using Qt Creator integrated debugging environment (IDE). GUI of the application is designed based on Qt Framework. Visual Studio 2015 C++ compiler is used to build the project on PC. Then the application is cross-built for Raspberry Pi 3 by using gcc-4.9-linaro-arm-gnueabi-hf toolchain.

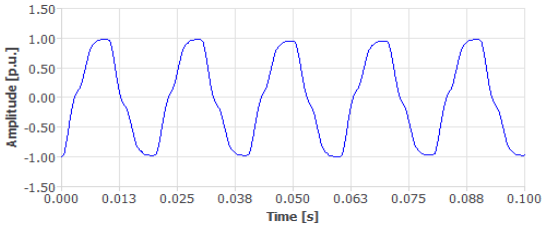

Figure 15. Signal with flicker

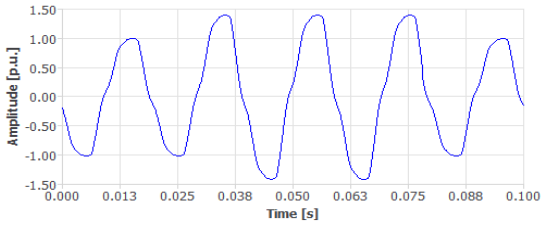

Figure 16. Signal with swell

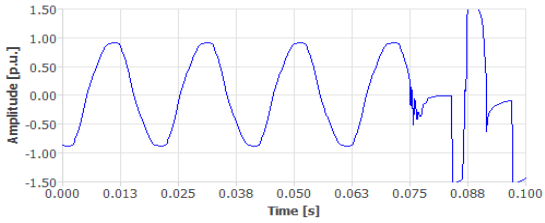

Figure 17. Signal with oscillatory transient

VI. Experimental Study

Performance measurement of the system is carried out by using 220 volts 50 Hz AC power voltage signal. Three potential transformers (PT) with 12 volts RMS seconder voltage are used to reduce the amplitude of the voltage on each phase. Divided seconder voltage (3.8 V) is applied to ADC inputs by using voltage divider connection (Fig. 18).

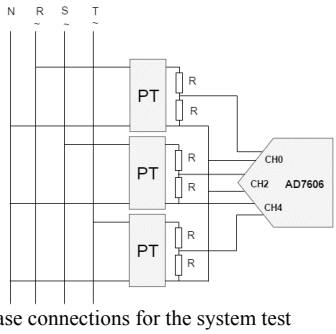

Figure 18. Three phase connections for the system test

The period of the observed line signal is 20 ms. The

application processes the acquired signal by accumulating 5 periods. Data reading and parsing, STA calculation, feature extraction, neural network classification, signal plotting and database record operations take time here. The application has to perform all these tasks in 100 ms in order to meet the real-time requirements. The elapsed timing measurements on a Raspberry Pi 3 single board computer are given in Table VII for 6 hours long operation.

TABLE VII. ELAPSED TIMING MEASUREMENTS DURING REAL-TIME PROCESSING

Operation (For Three Phase)	Elapsed Time (µs)		
	Minimum	Maximum	Mean
Signal Plotting	134	317	160
S-Transform (22x1000 double typed points) & Feature Extraction	13568	23687	14016
ANN computation	48	146	51
Database Record (5 cycles of raw data)	19160	215837	26294
TOTAL	32910	239987	**40521**

The sum of the mean processing times is under 41 ms and this result shows that the proposed system is sufficient for an admissible PQD detection system. The classification operation in [20] is completed in 71 ms for single phase without plotting and recording the signal data. Another paper [25] using DSP based hardware and decision tree for classification, reports a classification time about 90 ms for single phase operation. Authors of reference [15] report an ST computation time of 3.2 ms with fast dyadic scaling (dSPACE Application). However, this is a single-phase signal processing time with 640 sample points. Overall classification time is not reported within this paper. Reddy *et al.* [14] proposed a power quality monitoring system employing ST. In this study, ST is implemented with LabVIEW. The power signal is acquired with NI SCXI-1600 USB data acquisition device and ST 3D contours are displayed with the application. Nevertheless, automatic power quality classification task is not implemented within this study. Authors of this paper report a computation time of 0.75 s for only ST operation. As seen in the literature overview, the processing time required for PQD classification of the proposed ST scheme is lower than the previous implementations.

In our experiment, the database insertion operation takes the longest time and can be reduced by using an external storage device with higher write speed. For this experiment, Sandisk Ultra Dual drive with USB 3.0 OTG interface is used. However, Raspberry Pi 3 USB interface is USB 2.0 high speed compatible.

The data processing thread goes into the suspended state during the disk write operation and the data reader thread continues reading data from FIFO queue. Data overflow is avoided in this way. Database record operation is only performed when a PQ fault occurs, thus, the elapsed time for the raw signal record can be omitted. Another solution can be given as using "synchronous off" option for SQLite connection to decrease table insertion time. File write task is delivered to OS without waiting for completion with this option. On the other hand, this way is safe unless the power of processing computer gets interrupted. The mean times for processing is even under 5 ms on a notebook computer with Intel Core i7 3537U (3rd generation) CPU with 8 GB RAM and solid state drive.

VII. CONCLUSION

In this work, a USB interfaced power quality recognition and estimation system is implemented. The disturbance classification is realized by processing voltage signals of a three phase line. Power line voltage is acquired by using an FPGA powered multichannel simultaneous DAQ with USB-FIFO interface. Signal features regarding PQD are extracted by using ST. Feed forward back propagation ANN is used for the disturbance classification. Different from the previous studies, the harmonics measured in the real power signal, are added to synthetic signals which are used for training the ANN. Also, ST is performed over only the frequency lines used for the feature extraction. Seven features are used for classification. The ANN weights exported from MATLAB are used in the proposed application. Using pre-calculated weights makes the implementation become very practical. Additionally, acquired signal data are displayed in real-time. Performance measurement results validate that the proposed classification system is capable of detecting and logging power quality faults effectively in a real-time computing speed.

In our future work, a remote monitoring system will be integrated into this system by using Internet of things approach. Message Queuing Telemetry Transport (MQTT) protocol is a candidate method to build a distributed power grid monitoring system. MQTT protocol can be used both remote control and data collection purposes in a practical way.

REFERENCES

[1] S. Roy and S. Nath, "Classification of power quality disturbances using features of signals", International Journal of Scientific and Research Publications, vol. 2, no. 11, pp. 1-9, Nov. 2012.

[2] A. Rodriguez, J. Aguado, J. J. Lopez, F. I. Martin, F. J. Muñoz and J. E. Ruiz, Time-frequency transforms for classification of power quality disturbances, Power Quality, Intech, 2011, ch. 15. doi:10.5772/15397

[3] Y. Kong, J. Yuan, J. An and L. Che, "Online power quality disturbances detection and classification using one-pass Wavelet decomposition and Decision tree (Published Conference Proceedings style)" in Proceeding of Sixth International Conference on Machine Learning and Cybernetics, Hong Kong, 2007, pp. 2990-2995. doi:10.1109/ICMLC.2007.4370660

[4] S. Wei, H. Wen-fang, Y. Gui and D. Li-Fang, "Classification for power quality disturbances based on Cubic B-spline Wavelet and Decision tree", in International Conference on Computer Science and Software Engineering, Washington, 2008, pp. 823-826. doi:10.1109/CSSE.2008.809

[5] N. C. F. Tse, "Practical application of wavelet to power quality analysis (Published Conference Proceedings style)" in Proc. IEEE PES Gen. Meeting, Montreal, 2006, pp. 1–5. doi:10.1109/PES.2006.1709311

[6] J. Xu, S. Song and S. Shao, "Application in harmonics signal detection based on STFT and S Transform", Journal of Information and Computational Science, vol. 12, no. 9, pp. 3655-3664, Jun. 2015. doi: 10.12733/jics20105962

[7] M. Uyar, S. Yıldırım and M. T. Gencoglu, "An expert system based on S-transform and neural network for automatic classification of power quality disturbances", Expert Systems with Applications, vol. 36, no. 3, pp. 5962-5975, Apr. 2009. doi:10.1016/j.eswa.2008.07.030

[8] C. N. Bhende, S. Mishra and B. K. Panigrahi, "Detection and classification of power quality disturbances using S-Transform and Modular neural network", Electric Power Systems Research, vol. 78, no. 1, pp. 122-128, Jan. 2008. doi:10.1016/j.epsr.2006.12.011

[9] S. Kaewarsa, "Classification of power quality disturbance using S-Transform based artificial neural networks", in IEEE International

Conference on Intelligent Computing and Intelligent Systems, Shanghai, 2009, pp. 566-570. doi:10.1109/ICICISYS.2009.5357780

[10] M. Biswal and P. K. Dash, "Measurement and classification of simultaneous power signal patterns with an S-transform variant and fuzzy decision tree", IEEE Transactions on Industrial Informatics, vol. 9, no. 4, pp. 1819-1827, Nov. 2013. doi:10.1109/TII.2012.2210230

[11] A. Rodriguez, E. Merino, J. Aguado, J. J. Lopez, F. Muñoz, F. I. Martin and J. Muñoz, "A Decision tree and S-Transform based approach for power quality disturbances classification", In Fourth International Conference on Power Engineering, Energy and Electrical Drives (POWERENG), Istanbul, 2013, pp. 1093-1097. doi:10.1109/PowerEng.2013.6635763

[12] M. E. Salem, A. Mohamed and S. A. Samad, "Rule based system for power quality disturbance classification incorporating S-transform features", Expert Systems with Applications, vol. 37, no. 4, pp. 3229-3235, Apr. 2010. doi:10.1016/j.eswa.2009.09.057

[13] X. Xiao, F. Xu and H. Yang, "Short duration disturbance classifying based on S-transform maximum similarity", Electrical Power and Energy Systems, vol. 31, no. 7-8, pp. 374-378, Sept. 2009. doi:10.1016/j.ijepes.2009.03.006

[14] M. J. B. Reddy, K. Sagar and D. K. Mohanta, "A multifunctional real-time power quality monitoring system using Stockwell transform", IET Science, Measurement and Technology, vol. 8, no. 4, pp. 155-169, Jul. 2014. doi:10.1049/iet-smt.2013.0091

[15] M. Biswal and P. K. Dash, "Detection and characterization of multiple power quality disturbances with a fast S-transform and decision tree based classifier", Digital Signal Processing, vol. 23, no. 4, pp. 1071-1083, Jul. 2013. doi:10.1016/j.dsp.2013.02.012

[16] T. K. A. Galil, M. Kamel, A. M. Youssef, E. F. E. Saadany and M. M. A. Salama, "Power quality disturbance classification using the inductive inference approach", IEEE Transactions on Power Delivery, vol. 19 no. 10, pp. 1812–1818, Oct. 2004. doi:10.1109/TPWRD.2003.822533

[17] F. Zhao and R. Yang, "Power-Quality disturbance recognition using S-Transform", IEEE Transactions on Power Delivery, vol. 22, no. 2, pp. 944-950, Apr. 2007. doi:10.1109/TPWRD.2006.881575

[18] J. Li and M. V. Chilukuri, "Power supply quality analysis using S-Transform and SVM classifier", Journal of Power and Energy Engineering, vol. 2, no. 4, pp. 438-447, Apr. 2014. doi:10.4236/jpee.2014.24059

[19] A. Wang, F. Pan, Y. Li and R. Tao, "The design of power quality detecting system based of OMAP-L138", in IEEE 13th Workshop on Control and Modeling for Power Electronics, 2012, Kyoto, pp. 1-4. doi:10.1109/COMPEL.2012.6251732

[20] A. Rodriguez, J. A. Aguado, F. Martin, J. J. Lopez, F. Muñoz and J. E. Ruiz, "Rule-based classification of power quality disturbances using S-transform", Electric Power Systems Research, vol. 86, pp. 113-121, May 2012. doi:10.1016/j.epsr.2011.12.009

[21] Y. Chen, "Research and design of intelligent electric power quality detection system based on VI", Journal of Computers, vol. 5, no. 1, pp. 158-165, Jan. 2010. doi:10.4304/jcp.5.1.158-165

[22] T. Radil, P. M. Ramos, F. M. Janeiro and A. C. Serra, "PQ monitoring system for real-time detection and classification of disturbances in a single-phase power system", IEEE Transactions on Instrumentation and Measurement, vol. 57, no. 8, pp. 1725-1733, Aug. 2008. doi:10.1109/TIM.2008.925345

[23] R. Kumar, B. Singh, D. T. Shahani, A. Chandra and K. Al-Haddad, "Recognition of power quality disturbances using S-Transform-Based ANN classifier and rule-based Decision tree", IEEE Transactions on Industry Applications, vol. 51 no. 2, pp. 1249-1258, Mar. 2015. doi:10.1109/TIA.2014.2356639

[24] A. Miron, M. Dorin and A. C. Cziker, "Software tool for real-time power quality analysis", Advances in Electrical and Computer Engineering", vol. 13, no. 4, pp. 125-132, Nov. 2013. doi:10.4316/AECE.2013.04021.

[25] M. Zhang and K. Li, "DSP-FPGA based real-time power quality disturbances classifier", in IEEE PES Transmission and Distribution Conference and Exposition, 2010, New Orleans, pp. 1-6. doi:10.1109/TDC.2010.5484395

[26] X. She and J. Xiong, "Multi-channel electrical power data acquisition system Based on AD7606 and NIOSII", in International Conference on Electrical and Control Engineering, Yichang, 2011, pp. 1625-1627. doi:10.1109/ICECENG.2011.6057304

[27] M. Wang, G. I. Rowe and A. V. Mamishev, "Real-Time power quality waveform recognition with a programmable digital processor", in IEEE Power Engineering Society General Meeting, 2003, Toronto, pp. 1268-1273. doi:10.1109/PES.2003.1270511

[28] Z. He and Y. Liao, "The design of analog acquisition system in distribution automation", in 2012 China International Conference on Electricity Distribution (CICED), 2012, Shanghai, pp. 1-4. doi:10.1109/CICED.2012.6508437

[29] M. Gök, S. Görgünoğlu and İ. Sefa, "Design of a real-time USB interfaced multi-channel power system harmonics detection system", in 9th International Conference on Electrical and Electronics Engineering (ELECO), Bursa, 2015, pp. 521-524. doi:10.1109/ELECO.2015.7394539

[30] H. Guo, H. Yu, C. Sun, Z. Zhang and E. Zheng, "Continuous and real-time vibration data acquisition and analysis system based on S3C6410 and Linux", in Fifth Conference on Measuring Technology and Mechanism Automation, 2013, Hong Kong, pp. 389-392. doi:10.1109/ICMTMA.2013.98

[31] S. Shujing and L. Jiansheng, "A method of multi-channel data acquisition with adjustable sampling rate", *Telkomnika*, vol. 11, no. 9, pp. 5299-537, Sept. 2013.

[32] M. Caciotta, S. Giarnetti, F. Leccese, and D. Trinca, "Development of an USB data acquisition system for power quality and smart metering applications", in Proc. 11th International Conference on Environment and Electrical Engineering, Rome, 2012, pp. 835-839. doi:10.1109/EEEIC.2012.6221491

[33] R. G. Stockwell, L. Mansinha and R. P. Lowe, "Localization of the complex spectrum: The S Transform", IEEE Transactions on Signal Processing, vol. 44, no. 4, pp. 998-1001, Apr. 1996. doi:10.1109/78.492555

[34] S. He, K. Li and M. Zhang, "A real-time power quality disturbances classification using hybrid method based on S-Transform and dynamics", IEEE Transactions on Instrumentation and Measurement, vol. 62, no. 9, pp. 2465-2475, Sept. 2013. doi:10.1109/TIM.2013.2258761

[35] R. Hooshmand and A. Enshaee, "Detection and classification of single and combined power quality disturbances using fuzzy systems oriented by particle swarm optimization algorithm", *Electric Power Systems Research*, vol. 80, no. 12, pp. 1552-1561, Jul. 2010. doi:10.1016/j.epsr.2010.07.001

[36] B. Widrow, D. E. Rumelhard and M. A. Lehr, "Neural networks: Applications in industry, business and science", *Communication of ACM*, vol. 37, no. 3, pp. 93–105, Mar. 1994. doi:10.1145/175247.175257

[37] D. Borras, M. Castilla, N. Moreno and J. C. Montano, "Wavelet and neural structure: a new tool for diagnostic of power system disturbances", IEEE Transactions on Industry Applications, vol. 37, no. 1, pp. 184-190, Jan. 2001. doi:10.1109/28.903145

[38] S. Mishra, C. N. Bhende and B. K. Panigrahi, "Detection and classification of power quality disturbances using S-Transform and probabilistic neural network", IEEE Transactions on Power Delivery, vol. 23, no. 1, pp. 280-287, Jan. 2008. doi:10.1109/TPWRD.2007.911125

[39] I. W. C. Lee and P. K. Dash, "S-Transform based intelligent system for classification of power quality disturbance signals", IEEE Transactions on Industrial Electronics, vol. 50, no. 4, pp. 800-805, Aug. 2003. doi:10.1109/TIE.2003.814991

[40] M. V. Chilukuri and P. K. Dash, "Multiresolution S-Transform based fuzzy recognition system for power quality events", IEEE Transactions on Power Delivery, vol. 19, no. 1, pp. 323-330, Jan. 2004. doi:10.1109/TPWRD.2003.820180

[41] I. Škrjanc, S. Blažič and D. Matko, "Direct fuzzy model-reference adaptive control", International Journal of Intelligent Systems, vol. 17, no. 10, pp. 943-963, Oct. 2002. doi:10.1002/int.10054

[42] R. Precup and S. Preitl, "PI-fuzzy controllers for integral plants to ensure robust stability", Information Sciences, vol. 177, pp. 4410-4429, May 2007. doi:10.1016/j.ins.2007.05.005

[43] P. Moallem, B. S. Mousavi and S. Sh. Naghibzadeh, "Fuzzy inference system optimized by genetic algorithm for robust face and pose detection", International Journal of Artificial Intelligence, vol. 13, no. 2, pp. 73-88, Oct. 2015.

[44] J. Nowaková, M. Prilepok and V. Snásel, "Medical image retrieval using vector quantization and fuzzy S-tree", Journal of Medical Systems, vol. 41, no. 18, pp. 1-16, Feb. 2017. doi:10.1007/s10916-016-0659-2

[45] M. Frigo and S. G. Johnson, "FFTW: An adaptive software architecture for the FFT", in IEEE International Conference on Acoustics, Speech and Signal Processing, Seattle, 1998, pp. 1381-1384.